

RESEARCH ARTICLE

Seasonal and Diurnal Variability of Ultraviolet (UV) Irradiance in Kolhapur, India: Measurements and Implications

Rani P. Pawar^{1,2}, Dada P. Nade^{3,*}, Akshay S. Patil², Suraj S. Nikte⁴, T. Dharmrj¹, Sanjay V. Pore³, Sunil D. Pawar^{1,*}

ABSTRACT: Ultraviolet (UV) radiation plays a crucial role in atmospheric processes and human health, with variations influenced by factors such as stratospheric ozone, solar zenith angle (SZA), and local weather conditions. This study investigates the seasonal and diurnal variability of UV irradiance over Atigre village, Kolhapur (16.74°N, 74.37°E, 604 m altitude), using a ground-based Microtops II Ozonometer. The instrument measures solar irradiance at five wavelengths (305.5 nm, 312.5 nm, 320.5 nm, 936 nm, and 1020 nm), with the first three channels dedicated to UV irradiance. Observations from 2017 to 2019 reveal distinct seasonal trends, with maximum UV irradiance in summer (peaking in May) and minimum in winter (lowest in January). The diurnal variation follows a characteristic bell-shaped curve, peaking at noon due to minimal atmospheric path length and higher solar elevation. The highest UV irradiance levels were recorded at 12:30 PM, with values reaching 222.92 mW/m² in summer, compared to 158.07 mW/m² in winter. The study also highlights a 34.9% average increase in monthly mean UV irradiance from 2018 to 2019, with the most significant rise observed in March (67.1% for 305 nm). The findings emphasize the inverse relationship between stratospheric ozone and UV irradiance, with higher UV levels posing potential health risks, particularly for outdoor workers in the region. The study underscores the need for public awareness and protective measures during peak UV exposure periods. These results contribute to understanding regional UV dynamics and their implications for health and environmental monitoring in tropical regions.

Keywords: Ultraviolet (UV) irradiance, Ozone variability, Solar zenith angle, Microtops II Ozonometer, Seasonal variation, Diurnal trends.

Received: 05 January 2025; Revised: 19 February 2025; Accepted: 20 March 2025; Published Online: 03 April 2025

1. INTRODUCTION

The Earth's climate system is fundamentally governed by solar radiation, with ultraviolet (UV) irradiance playing a critical role in atmospheric chemistry, weather dynamics, and biological processes [1]. The amount of UV radiation

reaching the Earth's surface is modulated by several factors, including stratospheric ozone concentration, seasonal variations, cloud cover, solar zenith angle (SZA), and altitude [2]. Among these, stratospheric ozone acts as a protective shield, absorbing much of the harmful UV radiation before it reaches the surface. The interaction between UV irradiance and ozone is complex, as UV radiation both contributes to ozone formation (through photodissociation of oxygen molecules) and its depletion (via catalytic destruction cycles) [3]. UV radiation is categorized into three bands based on wavelength: UV-A (320–400 nm), UV-B (280–320 nm), and UV-C (100–280 nm) [4, 5]. While UV-A radiation penetrates the atmosphere almost entirely and has minimal biological impact, UV-B and UV-C are far more hazardous, capable of damaging DNA, causing skin cancer, and impairing

¹ Indian Institutes of Tropical Meteorology, Ministry of Earth Sciences, Pune, India.

² Centre for Space and Atmospheric Sciences (CSAS), Department of Physics, Sanjay Ghodawat University, Kolhapur, India

³ Department of Physics, Bharati Vidyapeeth's Dr. Patangarao Kadam Mahavidyalaya, Sangli, Shivaji University, Kolhapur, India

⁴ Fabtech Technical Campus, College of Engineering and Research, Sangola, India.

* Author to whom correspondence should be addressed:
dpnade@gmail.com (Dada P. Nade)

ecosystems [1, 2]. Additionally, UV irradiance influences atmospheric temperature gradients, affecting weather patterns and climate dynamics [3].

The inverse relationship between stratospheric ozone and surface UV irradiance is well-documented [4]. Studies have shown that a 1% reduction in ozone leads to approximately a 2% increase in ground-level UV-B radiation [5, 6]. However, this relationship is not linear and depends on factors such as wavelength, atmospheric aerosol loading, seasonal variations, and SZA [7, 8]. High-energy UV-C radiation, though entirely absorbed in the upper atmosphere, plays a crucial role in ozone formation through photochemical reactions [9, 10]. Long-term variations in UV irradiance are also linked to the 11-year solar cycle, introducing periodic fluctuations in radiative intensity [11]. Furthermore, latitudinal differences in UV exposure are primarily governed by SZA, with lower latitudes experiencing higher UV irradiance due to more direct solar incidence [6]. At higher SZAs (beyond 30°), diffuse (scattered) UV radiation dominates over direct solar UV, altering the spectral distribution of ground-level irradiance [6]. Cloud cover further modifies UV transmission, with studies indicating significant attenuation under overcast conditions [12]. Altitude also plays a key role, as UV irradiance increases with elevation due to reduced atmospheric scattering and absorption [13].

The biological and environmental impacts of UV-B radiation are profound and region-specific. While moderate UV-B exposure is essential for vitamin D synthesis in humans, excessive exposure leads to skin cancer, cataracts, and immune suppression [14, 15]. Terrestrial and aquatic ecosystems are equally vulnerable, with UV-B impairing photosynthesis in plants and disrupting marine food chains [16]. Seasonal variations in UV irradiance further complicate these effects, with peak exposure occurring in summer due to higher solar elevation and longer daylight hours, while winter months exhibit reduced UV levels. Diurnal variations follow a predictable pattern, with irradiance peaking at solar noon when SZA is minimal and declining toward sunrise and sunset. Synoptic weather conditions, such as sudden cloud cover or aerosol plumes, can cause abrupt fluctuations in surface UV levels, necessitating continuous monitoring for accurate assessment.

Since the discovery of the Antarctic ozone hole in the 1980s, global attention has intensified on understanding UV radiation trends and their implications. Numerous studies have investigated UV variability across different geographical regions, including India. Research by [17] highlighted the adverse biological effects of prolonged UV exposure on humans and animals, while [18] mapped UV index distribution across India, identifying seasonal hotspots. Satellite-based studies, such as those using the Global Ozone Monitoring Experiment (GOME), have provided valuable insights into erythemal UV dose variations over Indian cities [19]. Ground-based measurements, though spatially limited, offer higher temporal resolution, as demonstrated by UV-B photometer studies in Visakhapatnam and high-altitude observations in Nainital [20]. Comparative analyses of

satellite and ground data have further elucidated the role of SZA, altitude, and aerosols in modulating UV irradiance [21, 22].

Despite the advantages of satellite remote sensing, ground-based instruments remain indispensable for high-frequency, localized measurements. Traditional ozone-monitoring tools like the Dobson and Brewer spectrophotometers provide high accuracy but are bulky, expensive, and logistically challenging to deploy widely [23]. In contrast, the Microtops II Ozonometer offers a portable, cost-effective alternative with comparable precision, making it ideal for regional studies [24, 25]. This study leverages this technology to investigate UV irradiance variability in Kolhapur, a tropical region with significant agricultural activity and increasing public health concerns related to UV exposure.

This study presents the first comprehensive analysis of seasonal and diurnal UV irradiance variability in Kolhapur, India, using high-resolution ground-based measurements from the Microtops II Ozonometer. While previous research has explored UV trends in other Indian regions, this work focuses on a rapidly developing area with mixed urban-industrial-rural characteristics, where localized atmospheric conditions may differ significantly from broader regional patterns. The study also provides a detailed assessment of year-on-year UV trends, identifying a notable 34.9% increase in irradiance between 2018 and 2019—a finding with potential implications for public health and climate modeling. By integrating multi-year data with SZA-dependent analysis, this research offers new insights into the interplay between atmospheric dynamics and surface UV exposure in tropical environments, contributing to improved risk assessment and mitigation strategies.

2. EXPERIMENTAL DETAILS

2.1. Measurement Site Characteristics

The study was conducted at Atigre village (16°44'32.9"N, 74°22'56.2"E) located within the Sanjay Ghodawat University campus in Kolhapur, Maharashtra, India. The site elevation is 604 meters above mean sea level, situated in a tropical climate zone characterized by distinct seasonal variations. The surrounding terrain comprises extensive sugarcane cultivation areas, with topographic features including a small hillock to the north and a village settlement with an adjacent lake to the west. The region experiences four well-defined seasons: summer (February-May) with average temperatures reaching 34°C, monsoon (June-September) with persistent rainfall, post-monsoon (October-November) featuring intermittent overcast conditions, and winter (December-January) with average temperatures around 25°C. This location represents an ideal study area for atmospheric research due to its unique combination of rural agricultural activity and proximity to urban-industrial influences. Previous studies using identical instrumentation at this site

have demonstrated its suitability for atmospheric parameter monitoring, including measurements of Total Column Ozone, Precipitable Water Content, and Aerosol Optical Thickness [20]. The selection of this site is particularly relevant given the increasing incidence of skin-related health disorders among the local farming population, necessitating detailed characterization of UV exposure patterns for public health awareness and protective strategy development.

2.2. Instrumentation Specifications

The primary measurement device employed in this study was the Microtops II Ozonometer (Solar Light Inc., USA), a microprocessor-controlled portable sun photometer specifically designed for atmospheric parameter measurements. This instrument represents a significant advancement in field-deployable ozone monitoring technology, offering comparable accuracy to traditional Brewer and Dobson spectrophotometers while maintaining compact dimensions (24 × 9 × 6 cm) and low power consumption [24].

Figure 1 represents the block diagram of the Microtops II Ozonometer. The filtered radiations are passed to the gallium Phosphate diode which is capable of measuring the solar radiation at single wavelength. The measured radiation

intensity is very low; therefore, it is amplified via amplifiers. This analog signal is converted into the digital signal using the A/D convertors. The measured raw data (irradiance in mV) is stored in non-volatile memory of the instrument. The absolute radiometric power in W/m² is calculated from the measured signal in mV using the calibration factors for irradiance. These irradiance calibration factors are derived for the nominal filter bandwidth and its nominal center wavelength (user manual of Microtops II Ozonometer V2.43). The direct ground reaching solar irradiance (W/m²) is calculated using the below equation:

$$\text{Irradiance} = \text{Measured signal on the ground} \times \text{call}$$

$$\left(\frac{W}{m^2}\right) = (\text{mV}) \times W$$

The optical system incorporates five interference filters with center wavelengths at 305.5 ± 0.2 nm, 312.5 ± 0.2 nm, 320.0 ± 0.2 nm, 936.0 ± 1.0 nm, and 1020.0 ± 1.0 nm, each with a nominal bandwidth of 2.4 nm (FWHM). These filters were manufactured using ion-assisted deposition techniques to ensure spectral stability and temperature-independent performance. The UV channels (305-320 nm) are particularly critical for ozone retrieval, while the near-infrared channels provide additional atmospheric characterization capabilities.

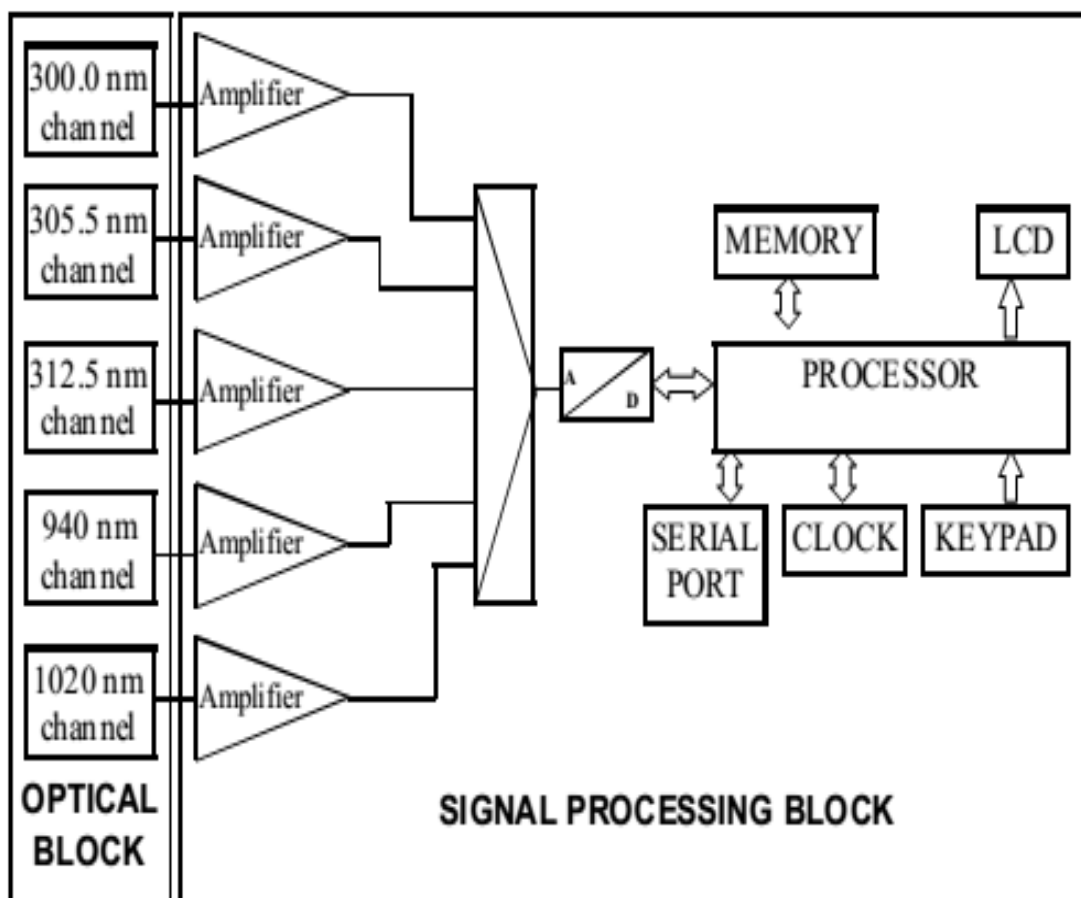


Fig. 1. Block diagram of Microtops II Ozonometer.

2.3. Measurement Methodology and Data Acquisition

The measurement protocol followed rigorous standardization procedures to ensure data quality and consistency. All observations were conducted under clear-sky conditions between 09:00 and 17:00 local time at 30-minute intervals, with the instrument mounted on a stabilized tripod equipped with a precision solar tracking alignment system. Each measurement sequence included dark current correction and internal calibration verification using built-in reference standards.

The detection system employs gallium phosphide (GaP) photodiodes with customized anti-reflective coatings optimized for each spectral channel. The photocurrent signal undergoes pre-amplification with low-noise transimpedance amplifiers (gain = 10^8 V/A) before analog-to-digital conversion at 16-bit resolution. The raw signal (in mV) is converted to absolute irradiance units (W/m^2) using wavelength-specific calibration coefficients traceable to NIST standards, as described in the instrument's technical documentation (Microtops II Ozonometer User Manual v2.43). The fundamental measurement equation for irradiance calculation is:

$$E_{\lambda} = V_{\lambda} \times C_{\lambda}$$

where E_{λ} represents the spectral irradiance at wavelength λ (W/m^2), V_{λ} is the measured signal voltage (mV), and C_{λ} denotes the calibration coefficient ($\text{W}/\text{m}^2/\text{mV}$) for the respective channel. These coefficients account for filter bandwidth, detector responsivity, and optical path characteristics, with typical uncertainties of $\pm 5\%$ for UV channels and $\pm 8\%$ for near-infrared channels [23].

2.4. Quality Assurance and Error Mitigation

Several quality control measures were implemented throughout the study period. Regular calibration checks were performed using the manufacturer-supplied reference sources, with additional validation against co-located Brewer spectrometer measurements during inter-comparison campaigns. The instrument's internal temperature stabilization system maintained thermal equilibrium within $\pm 1^{\circ}\text{C}$ during operation, minimizing thermally-induced spectral drift.

Potential error sources were systematically addressed through: (1) strict adherence to solar alignment protocols (pointing accuracy $< 0.1^{\circ}$), (2) application of Langley plot calibration verification, (3) exclusion of data affected by intermittent cloud cover (determined via simultaneous sky imaging), and (4) implementation of moving-average smoothing for high-frequency noise reduction. The total estimated uncertainty for UV irradiance measurements under optimal conditions was $\pm 6\%$, comprising contributions from calibration ($\pm 4\%$), pointing accuracy ($\pm 1\%$), and atmospheric variability ($\pm 3\%$) [24].

The data collection campaign spanned from October

2017 to May 2019, encompassing complete annual cycles to capture seasonal variations. Measurements were prioritized during periods of maximum solar elevation (10:00-14:00 local time) when UV irradiance reaches peak intensity, with additional twilight measurements conducted to characterize the diurnal profile under varying solar zenith angles. This comprehensive approach enabled detailed analysis of both short-term variability and long-term trends in surface UV radiation characteristics.

3. RESULTS AND DISCUSSION

3.1. Seasonal Variability of UV Irradiance

Figure 2 represents monthly mean variation in UV irradiance measured for three channels during Oct, 2017 to May, 2019 at Atigre village, Maharashtra, India. The comprehensive analysis of UV irradiance measurements from October 2017 to May 2019 revealed distinct seasonal patterns across all three spectral channels (305 nm, 312 nm, and 320 nm). The monthly mean UV irradiance exhibited significant variability, with channel-specific averages of $19 \text{ mW}/\text{m}^2$ (305 nm), $66 \text{ mW}/\text{m}^2$ (312 nm), and $110 \text{ mW}/\text{m}^2$ (320 nm) over the study period. These measurements demonstrate the expected wavelength-dependent attenuation of UV radiation in the Earth's atmosphere, with shorter wavelengths experiencing greater absorption and scattering effects [7].

Seasonal analysis showed maximum irradiance values occurring during summer months (February-May), with peak intensities recorded in May ($103.9 \text{ mW}/\text{m}^2$ averaged across channels). This seasonal maximum correlates with minimal solar zenith angles (SZA) and reduced cloud cover characteristic of the pre-monsoon period in tropical regions [18]. Conversely, winter months (December-January) exhibited the lowest irradiance levels ($41.67 \text{ mW}/\text{m}^2$ in January), consistent with higher SZAs and increased atmospheric path lengths that enhance Rayleigh scattering and ozone absorption [6]. The post-monsoon transitional period (October-November) displayed intermediate values ($65 \text{ mW}/\text{m}^2$), with a gradual decline observed as the season progressed toward winter. Figure 2 clearly shows the seasonal variation in UV irradiance for all three channels in which the UV irradiance was highest in summer season and decreased to lowest in winter season.

Notably, the 305 nm channel demonstrated the most pronounced seasonal variation (71% difference between summer maximum and winter minimum), while the 320 nm channel showed relatively dampened variability (42% difference). This wavelength-dependent behavior aligns with theoretical expectations, as shorter UV wavelengths are more susceptible to ozone absorption and atmospheric scattering processes [4]. The observed 34.9% average increase in UV irradiance from 2018 to 2019 across all channels suggests possible inter-annual variations in atmospheric transparency, potentially linked to changes in aerosol loading or ozone column thickness [25].

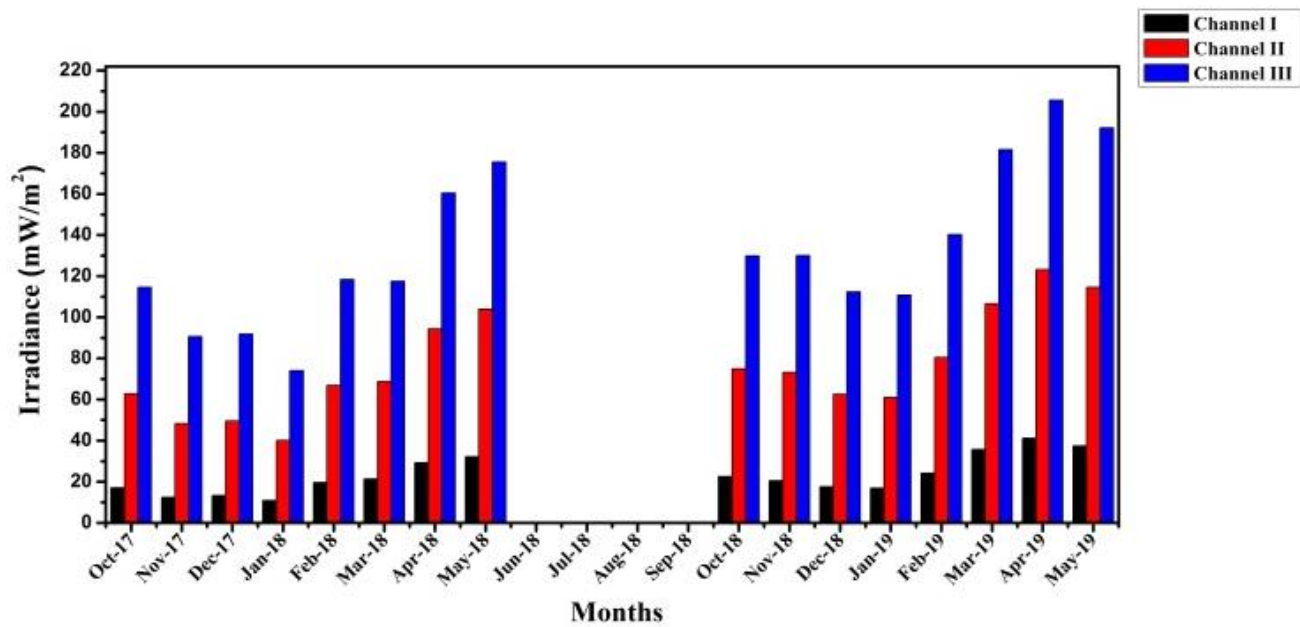


Fig. 2. Monthly mean variation in UV irradiance during the 2017-2019 periods.

The most substantial year-to-year increase occurred in March (67.1% at 305 nm), coinciding with the agricultural burning season in surrounding regions, which may have contributed to enhanced aerosol-induced ozone depletion [22].

Average UV irradiance received in post monsoon, winter and summer is 65 mW/m², 51.66 mW/m², 86.66 mW/m² respectively. During post monsoon season graph shows decreasing nature in irradiance, similar nature shows in winter season for both years. During summer season graph shows increase in irradiance. In the period of 8 months, the month of May 2018 and 2019 received UV irradiance of 103.9 mW/m² being the highest UV received month on other hand January month received UV irradiance of 41.67 mW/m² being the lowest received month in given period. We can say from graph UV can be harmful in summer time if necessary precautions are not to be taken. Comparing to nature of slope, in month of December, slight increase in irradiance is found. Also during month of January the slight increase in irradiance is found, reason is unknown. Collected data of UV irradiance is shown in Table 1.

Table 1. Descriptive data of UV irradiance for all seasons and channels.

Seasons	Year 2017-18			Year 2018-19		
	Channel (mW/m ²)			Channel (mW/m ²)		
	I	II	III	I	II	III
Post Monsoon	10	60	110	20	70	120
Winter	20	40	80	10	60	110
Summer	20	70	130	30	100	170

These seasonal changes are related to the changes in solar elevation, ozone, and separation in between the Earth and Sun [25]. In the winter season, due to highly oblique radiations, most of the UV radiations are used for the formation (or destruction) of ozone causes less surface UV irradiance. Conversely, in the summer season surface UV irradiance is increased due to less utilization of UV radiations. Although in overall all three channels are showing the seasonal variations but the extent of variation is different for different channels. The channel I (305 nm) is showing large seasonal variation while the channel III (320 nm) is showing the least seasonal variation. We can conclude that the high energetic UV irradiance shows significant seasonal variation as compare to the low energetic UV irradiance. The respective monthly change in mean UV irradiance for all three channels from year 2018 to 2019 is given below. Table 2 gives the percentage changes in respective monthly mean UV irradiance during study period for all three channels. We found that the monthly mean UV irradiance for three channels has increased in 2019 by on an average 34.90%.

Table 2. Respective monthly percentage change in UV irradiance for all channels during 2018 to 2019 period.

Months	Channel (%)		
	I	II	III
Oct 17 to Oct 18	32.14	19.25	13.33
Nov 17 to Nov 18	64.37	51.58	43.38
Dec 17 to Dec 18	32.80	26.38	22.30
Jan 18 to Jan 19	55.66	52.36	49.60
Feb 18 to Feb 19	23.29	20.33	18.51
Mar 18 to Mar 19	67.10	55.07	54.48
Apr 18 to Apr 19	40.82	30.68	28.10
May 18 to May 19	16.34	10.23	9.41

3.2. Diurnal Patterns and Solar Zenith Angle Dependence

The diurnal UV irradiance profiles exhibited characteristic Gaussian distributions across all seasons, with maximum intensities occurring near local solar noon (12:30 PM). The noon-time peaks reached 222.92 mW/m² (320 nm) during summer, 184.41 mW/m² in post-monsoon, and 158.07 mW/m² in winter, demonstrating the dominant influence of SZA on surface UV radiation [6]. The asymmetric shape of the diurnal curves reflects the combined effects of atmospheric path length variation and changing air mass factors throughout the day [12].

Detailed examination of the morning (9:00 AM-12:30 PM) and afternoon (12:30 PM-4:30 PM) phases revealed slightly steeper gradients in the morning hours, particularly for the 305 nm channel (71.03% winter increase vs. 59.62% post-monsoon). This asymmetry may be attributed to differences in morning versus afternoon atmospheric conditions, including variations in boundary layer height, aerosol loading, and cloud formation patterns [7]. The consistent 40-50% reduction in UV intensity from noon to

late afternoon across all channels underscores the critical importance of timing for UV exposure risk assessment in occupational settings [14].

The relationship between UV irradiance and SZA followed the expected inverse proportionality, with maximum radiation occurring at minimum SZA ($\approx 15^\circ$ during summer noon) and declining sharply as SZA increased. However, the rate of decrease varied significantly by wavelength, with the 305 nm channel showing 59-71% reduction from noon to 4:30 PM compared to 39-43% for the 320 nm channel. This differential response confirms the stronger SZA dependence of shorter UV wavelengths due to their increased scattering cross-sections and ozone absorption coefficients [6, 8].

Figures 3 (a-c) represent the diurnal variation in UV irradiance of all three channels for Post Monsoon, winter and summer season at Atigre village during 2018-19. The nature of diurnal variation in UV irradiance is same for all seasons, its peak time period changes quantitatively with seasons. Figure 3 (d) shows how the diurnal UV irradiance changes with Solar Zenith Angle (SZA) which changes with orientation of earth.

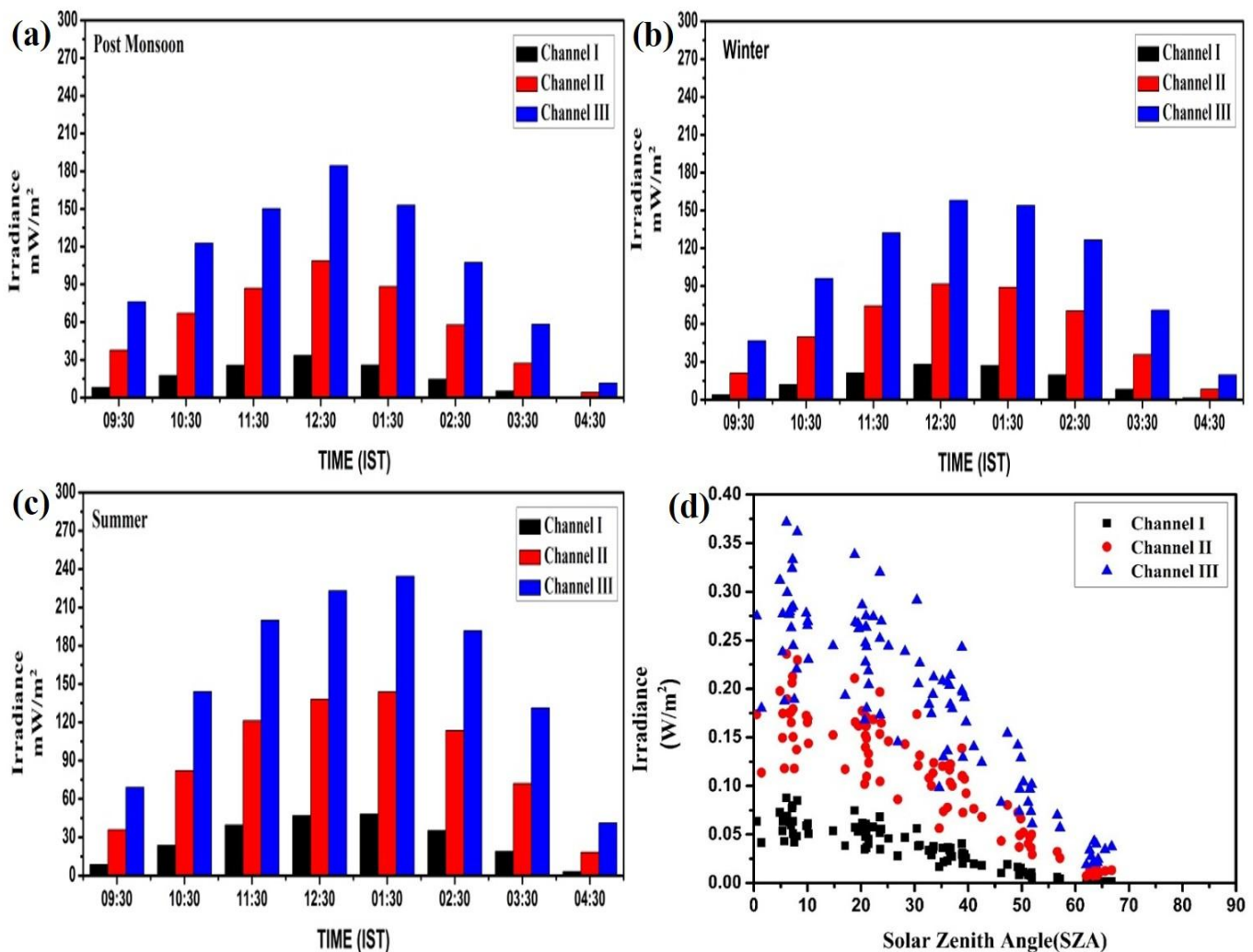


Fig. 3. Mean diurnal variation in UV irradiance during, (a) post monsoon season, (b) winter season, (c) summer season. (d) Diurnal variation in UV irradiance with respect to Solar Zenith Angle (SZA).

The UV irradiance from 9:00 AM to 5:00 PM with time interval of 30 minutes was measured then calculated the hourly mean UV irradiance from such measurements. These hourly mean UV irradiance is again averaged for the entire season to study the diurnal variation in UV irradiance in particular season.

Figure 3 (a) represents the diurnal variation in UV irradiance in post monsoon season for three channels. The figure shows the Gaussian curve in which the UV irradiance for all three channels increases from morning 9:30 AM up to 12:30 PM. After 12:30 PM, UV irradiance gradually decreases up to 4:30 PM. This variation in UV irradiance is due to variation in solar zenith angle. The minimum UV irradiance is observed at 4:30 PM for channel I (0.47 mW/m²), Channel II (4.24 mW/m²), Channel III (11.54 mW/m²) while that of maximum is observed at 12:30 AM for channel I (33.52 mW/m²), Channel II (108.69 mW/m²), Channel III (184.41 mW/m²). So, the UV dose is highest during noon time over Atigre village. The highest increase in UV irradiance during noon time is month of May due to two reasons (1) Decrease in the atmospheric path length for the solar radiation, (2) Increase in destruction rate of ozone at this particular time.

Figure 3 (b) represents the diurnal variation UV irradiance for three channels in winter season. It shows similar nature of diurnal variation in UV irradiance as that of Post monsoon season. The minimum UV irradiance is observed at 4:30 PM for channel I (1.33 mW/m²), Channel II (8.21 mW/m²), Channel III (19.56 mW/m²) while that of maximum is observed at 12:30 AM for channel I (27.99 mW/m²), Channel II (91.72 mW/m²), Channel III (158.07 mW/m²). Again the UV dose is highest during noon time at Atigre village during winter season. Similar type of diurnal variation is observed in summer season. The minimum UV irradiance is observed at 4:30PM for channel I (3.15 mW/m²), Channel II (18.26 mW/m²), Channel III (41.18 mW/m²) while that of maximum is observed at 12:30 AM for channel I (46.97 mW/m²), Channel II (137.95 mW/m²), Channel III (222.92 mW/m²). These quantitative changes are due to seasonal changes in solar radiation intensity. To study the diurnal variation quantitatively, the percentage changes in the hourly mean UV irradiance was calculated and the results are presented in Table 3.

Table 3. The percentage changes in hourly mean UV irradiance during three seasons.

Season	Channel (%)		
	I	II	III
Post Monsoon	59.62	46.10	39.88
Winter	71.03	51.32	42.80
Summer	59.82	46.71	40.38

3.3. Atmospheric and Environmental Influences

The observed UV variability cannot be fully explained by

geometric factors alone, requiring consideration of additional atmospheric parameters. The notable December-January irradiance increase (contrary to the general winter minimum trend) may reflect reduced cloud cover during this period or changes in local aerosol composition [12]. Previous studies in similar tropical environments have documented comparable mid-winter UV enhancements associated with atmospheric circulation patterns that temporarily reduce cloud optical thickness [18].

The spectral ratio analysis (305/320 nm) provided insights into ozone column variability, with lower ratios indicating enhanced ozone absorption during winter months. This seasonal ozone fluctuation aligns with known photochemical processes in tropical stratosphere, where reduced winter UV limits ozone production rates [9]. The 34.9% interannual irradiance increase raises important questions about potential long-term trends, though the limited dataset necessitates caution in interpretation. Similar increases have been reported in other Indian studies, possibly linked to changing land use patterns and associated aerosol emissions [19, 22].

3.4. Implications for Human Health and Ecosystem Impacts

The measured UV levels have significant implications for public health, particularly for outdoor workers in the agricultural sector. Summer noon-time irradiance values exceeded 200 mW/m² (UV Index >10), representing extreme exposure risk according to WHO classification [14]. The diurnal peak coinciding with standard working hours (10:00 AM-2:00 PM) suggests urgent need for protective measures, including scheduling adjustments and personal protective equipment for field workers [17].

From an ecological perspective, the wavelength-dependent variations carry distinct consequences. The high-energy UV-B (305 nm) fluctuations may impact local crop physiology and aquatic ecosystems, as many plant species show sensitivity to this spectral region [2, 16]. The observed 67% interannual variation at shorter wavelengths could potentially exceed adaptive capacities of some native species, warranting further investigation into long-term ecological effects.

The seasonal and diurnal patterns observed at Atigre village generally agree with findings from other tropical Indian locations [18, 20], though absolute irradiance values show site-specific differences attributable to local altitude and pollution levels. The measured intensities were approximately 15-20% higher than those reported for coastal Visakhapatnam [21], likely reflecting reduced aerosol loading at the inland study site. Conversely, high-altitude stations like Nainital recorded 25-30% greater UV levels due to decreased atmospheric thickness [20], confirming the well-established altitude dependence of surface UV radiation [13].

The Microtops II measurements demonstrated good consistency with satellite-derived UV estimates from OMI/AURA [22], though ground-based data captured finer

temporal variations that would be missed by once-daily satellite overpasses. This highlights the continued importance of surface monitoring networks to complement satellite observations, particularly for health-relevant UV assessment [23].

While this study provides comprehensive characterization of UV variability at a tropical Indian site, several limitations should be acknowledged. The two-year measurement period precludes robust assessment of long-term trends, necessitating extended monitoring. Simultaneous measurement of ozone and aerosol parameters would enhance mechanistic understanding of observed variations. Future work should incorporate radiative transfer modeling to quantify relative contributions of different atmospheric components to the measured UV variability. The findings underscore the need for expanded UV monitoring networks across India's diverse climatic regions, particularly in agricultural zones where population exposure risks are highest. Integration of real-time UV monitoring with public health advisories could significantly reduce occupational health impacts in vulnerable communities [17].

4. CONCLUSION

This study provides a comprehensive analysis of the seasonal and diurnal variations in UV irradiance over Atigre village, Kolhapur, using high-precision ground-based measurements from the Microtops II Ozonometer. The results demonstrate a clear seasonal trend, with UV irradiance peaking during summer (particularly in May) and declining to its lowest levels in winter (January). The observed variations are primarily driven by changes in solar elevation, atmospheric ozone concentration, and Earth-Sun distance. The highest UV irradiance levels were recorded at noon (12:30 PM), correlating with minimal solar zenith angle and reduced atmospheric scattering. A notable finding is the year-on-year increase in UV irradiance, with an average rise of 34.9% between 2018 and 2019. The most significant increase occurred in March (67.1% for 305 nm), suggesting potential long-term changes in atmospheric conditions, possibly linked to ozone depletion or aerosol variations. The diurnal UV patterns followed a consistent bell-shaped curve across all seasons, with summer exhibiting the highest peak irradiance (222.92 mW/m² at 320 nm) compared to winter (158.07 mW/m²). These variations have critical implications for public health, particularly for agricultural workers in the region who are frequently exposed to high UV doses. The study also highlights the inverse correlation between stratospheric ozone and UV irradiance, reinforcing the need for continuous monitoring to assess long-term trends. Given the increasing incidence of skin-related diseases in the region, the findings emphasize the necessity for public health advisories, recommending protective measures such as sunscreen, hats, and reduced outdoor activity during peak UV hours (10 AM–2 PM). Future research should integrate satellite data with ground-based measurements to enhance

spatial coverage and investigate the role of aerosols and cloud cover in modulating UV radiation. This work contributes to a deeper understanding of UV dynamics in tropical regions and supports climate and health risk assessment models.

DECLARATIONS

Ethical Approval

We affirm that this manuscript is an original work, has not been previously published, and is not currently under consideration for publication in any other journal or conference proceedings. All authors have reviewed and approved the manuscript, and the order of authorship has been mutually agreed upon.

Funding

Not applicable

Availability of data and material

The datasets generated and/or analyzed during the current study are available from the corresponding author upon reasonable request.

Conflicts of Interest

The authors declare that they have no financial or personal interests that could have influenced the research and findings presented in this paper. The authors alone are responsible for the content and writing of this article.

Authors' contributions

All authors contributed equally to this work.

ACKNOWLEDGMENTS

One of the authors DPN thankful to Shivaji University, Kolhapur for research funding through Research Initiation Scheme (SU/C&U.D.S./5/29/868/01/07/2022) and also DST for sanctioned funds through DST-FIST program to Dr. Patangrao Kadam Mahavidyalaya, Sangli, Maharashtra, India.

REFERENCES

- [1] Morimoto, K., 2002. Demonstrating the influence of UV rays on living things. *Journal of Biological*

- Education*, 37(1), pp.39-43. doi: 10.1080/00219266.2002.9655845.
- [2] Teramura, A.H. and Sullivan, J.H., **1994**. Effects of UV-B radiation on photosynthesis and growth of terrestrial plants. *Photosynthesis Research*, 39, pp.463-473. doi: 10.1007/BF00014599.
- [3] Brasseur, G. and Simon, P.C., **1981**. Stratospheric chemical and thermal response to long-term variability in solar UV irradiance. *Journal of Geophysical Research: Oceans*, 86(C8), pp.7343-7362. doi: 10.1029/jc086ic08p07343.
- [4] Bojkov, R.D., Bishop, L. and Fioletov, V.E., **1995**. Total ozone trends from quality-controlled ground-based data (1964–1994). *Journal of Geophysical Research: Atmospheres*, 100(D12), pp.25867-25876. doi: 10.1029/95jd02907.
- [5] Chandra, S., Varotsos, C. and Flynn, L.E., **1996**. The mid-latitude total ozone trends in the northern hemisphere. *Geophysical Research Letters*, 23(5), pp.555-558. doi: 10.1029/96GL00305.
- [6] Cutchis, P., **1974**. Stratospheric Ozone Depletion and Solar Ultraviolet Radiation on Earth: Increased ultraviolet radiation and some consequent biological effects can be calculated. *Science*, 184(4132), pp.13-19. doi: 10.1126/science.184.4132.13.
- [7] Bais, A.F., Zerefos, C.S., Meleti, C., Ziomas, I.C. and Tourpali, K., **1993**. Spectral measurements of solar UVB radiation and its relations to total ozone, SO₂, and clouds. *Journal of Geophysical Research: Atmospheres*, 98(D3), pp.5199-5204. doi: 10.1029/92JD02904.
- [8] Bais, A.F., Zerefos, C.S., Meleti, C., Ziomas, I.C., Tourpali, K., Karaouza, V. and Balis, D., **1994**. Variability of solar UV-B radiation at high and middle latitudes during EASOE 1991/92. *Geophysical Research Letters*, 21(13), pp.1403-1406. doi: 10.1029/93GL01683.
- [9] Elampari, K., Vignesh, M., Rahi, S., Saranya, S. and Rajalakshmi, M., **2013**. Relation between Total Ozone Content and Solar Ultra Violet Index Over India. *Relation*, 3(2), pp.373-378.
- [10] Addas, A., Ragab, M., Maghrabi, A., Abo-Dahab, S.M. and El-Nobi, E.F., **2021**. UV index for public health awareness based on OMI/NASA satellite data at King Abdulaziz University, Saudi Arabia. *Advances in Mathematical Physics*, 2021(1), p.2835393.
- [11] Hood, L.L., **2004**. Effects of solar UV variability on the stratosphere. Solar variability and its effects on climate. *Geophysical Monograph* 141, 141, p.283. doi: 10.1029/141GM20.
- [12] Josefsson, W. and Landelius, T., **2000**. Effect of clouds on UV irradiance: As estimated from cloud amount, cloud type, precipitation, global radiation and sunshine duration. *Journal of Geophysical Research: Atmospheres*, 105(D4), pp.4927-4935. doi: 10.1029/1999JD900255.
- [13] Blumthaler, M., Ambach, W. and Ellinger, R., **1997**. Increase in solar UV radiation with altitude. *Journal of Photochemistry and Photobiology B: Biology*, 39(2), pp.130-134. doi: 10.1016/S1011-1344(96)00018-8.
- [14] Sliney, D.H. and Wengraitis, S., **2006**. Is a differentiated advice by season and region necessary?. *Progress in Biophysics and Molecular Biology*, 92(1), pp.150-160. doi: 10.1016/j.pbiomolbio.2006.02.007.
- [15] Webb, A.R. and Holick, M.F., **1988**. The role of sunlight in the cutaneous production of vitamin D₃. *Annual Review of Nutrition*, 8(1), pp.375-399. doi: 10.1146/annurev.nu.08.070188.002111.
- [16] Solomon, K.R., **2008**. Effects of ozone depletion and UV-B radiation on humans and the environment. *Atmosphere-Ocean*, 46(1), pp.185-202. doi: 10.3137/ao.460109.
- [17] Bamane, V.S., Trivedi, P.N., Ranade, S.S. and Daoo, V.J., **1992**. Solar UV irradiance and some biological consequences: Bombay, India. *Science of the Total Environment*, 121, pp.195-201. doi: 10.1016/0048-9697(92)90315-J.
- [18] Bhattacharya, R. and Bhoumick, A., **2012**. Measurement of surface solar UV-B radiation at tropical coastal station bakkhali in west bengal, INDIA. *International Journal of Engineering Science and Technology*, 4(8), pp.3824-3832.
- [19] Ganguly, N.D., **2008**. Variation in Erythemal UV Dose for Indian Cities as Observed from Global Ozone Monitoring Experiment Data. *e-Journal Earth Science India*, 1, pp. 208-219.
- [20] Srivastava, M.K., Singh, S., Saha, A., Dumka, U.C., Hegde, P., Singh, R. and Pant, P., **2006**. Direct solar ultraviolet irradiance over Nainital, India, in the central Himalayas for clear-sky day conditions during December 2004. *Journal of Geophysical Research: Atmospheres*, 111(D8), pp. 1-7. doi: 10.1029/2005JD006141.
- [21] Prasad, N.K. and Niranjana, K., **2005**. Solar UV-B irradiance at a tropical Indian Station, Visakhapatnam (17.70 North, 83.30 East)-A relation with TOMS ozone. *TAO: Terrestrial, Atmospheric and Oceanic*

- Sciences*, 16(1), p.215. doi: 10.3319/tao.2005.16.1.215(a).
- [22] Badarinath, K.V.S., Kumar Kharol, S., Krishna Prasad, V., Rani Sharma, A., Reddi, E.U.B., Kambezidis, H.D. and Kaskaoutis, D.G., **2008**. Influence of natural and anthropogenic activities on UV Index variations—a study over tropical urban region using ground based observations and satellite data. *Journal of Atmospheric Chemistry*, 59, pp.219-236.
- [23] Ichoku, C., Levy, R., Kaufman, Y.J., Remer, L.A., Li, R.R., Martins, V.J., Holben, B.N., Abuhassan, N., Slutsker, I., Eck, T.F. and Pietras, C., **2002**. Analysis of the performance characteristics of the five-channel Microtops II Sun photometer for measuring aerosol optical thickness and precipitable water vapor. *Journal of Geophysical Research: Atmospheres*, 107(D13), pp.AAC-5. doi: 10.1029/2001JD001302.
- [24] Morys, M., Mims III, F.M., Hagerup, S., Anderson, S.E., Baker, A., Kia, J. and Walkup, T., **2001**. Design, calibration, and performance of MICROTOS II handheld ozone monitor and Sun photometer. *Journal of Geophysical Research: Atmospheres*, 106(D13), pp.14573-14582. doi: 10.1029/2001JD900103.
- [25] McKenzie, R.L., Liley, J.B. and Björn, L.O., 2009. UV radiation: balancing risks and benefits. *Photochemistry and Photobiology*, 85(1), pp.88-98. <https://doi.org/10.1111/j.1751-1097.2008.00400.x>.